ACS OMEGA

Article

Cite This: ACS Omega 2018, 3, 10974−10979

http://pubs.acs.org/journal/acsodf

Convenient and Template-Free Route to One-Pot Green Synthesis of Polyrhodanine Core−Shell Nanoparticles

Moni Chauhan,*[,†] Anjali Gaba,[†] Tao Hong,[†] Evens Esperance,[†] Qiaxian Johnson,[‡] Gurjeet Longia,[‡] and Bhanu P. S. Chauhan*[,‡]

[†]Department of Chemistry, Queensborough Community College of City University of New York, Bayside, New York 11364, United States

[‡]Engineered Nanomaterials Laboratory, Department of Chemistry, William Patterson University, 300 Pompton Road, Wayne, New Jersey 07470, United States

Supporting Information

ABSTRACT: In this publication, a copper acetate-mediated rhodanine polymerization reaction is examined. It is demonstrated that at room temperature, Cu(II) acetate complexes with rhodanine generate solid nanospheres, which, upon heating in a microwave, results in polyrhodanine core−shell nano- and microsphere particles. The structural analysis of the polyrhodanine nanosphere produced by this efficient microwave-initiated method was conducted by Fourier transform infrared spectroscopy, UV−vis spectroscopy, scanning electron microscopy, and transmission electron microscopy. In addition, it is verified that this template-free, efficient, and versatile synthesis of polyrhodanine nanospheres can also be accomplished by introducing a strong oxidant $KMnO_4$ as a cocatalyst with copper acetate without compromising the morphology of the resulting core−shell nanospheres. It is also demonstrated that the polyrhodanine nanospheres can be used to adsorb methyl orange dye, a known contaminant in industrial wastewater.

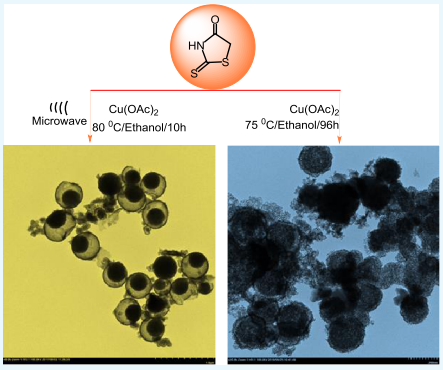

1. INTRODUCTION

The conjugation of conducting polymers (polypyrrole, polyaniline, polythiophene, and polyrhodanine) with inorganic complexes provides materials with promising and attractive properties for their application in new and diverse technologies.[1] In recent years, rhodanine (Rh) and its derivatives have attracted attention because of their antibacterial, antiviral, antihistaminic, and anticorrosion properties.[2] Electrochemically synthesized high-quality polyrhodanine (pRh) films prepared by Kardaş and co-workers[3] and silver/pRh nanotubes and nanofiber composite materials synthesized by Jang and co-workers[3] exhibit a very high antimicrobial efficacy against Gram-negative and Gram-positive bacteria and yeast. A green approach to the cellulose nanocrystal Fe(III) complex-coated pRh in aqueous medium and silica-coated pRh/silver nanocomposite exhibits sustainable antimicrobial properties for applications in food packaging, antimicrobial coatings, and additives.[4] It has also been demonstrated that the pRh-immobilized anodic aluminum oxide membrane fabricated via vapor deposition polymerization can chemically absorb metals like Ag(I), Hg(II), and Pb(II) ions, and the pRh/isobutyltriethoxysilane films can effectively hinder the access of chloride ions to the stainless steel surface providing anticorrosion properties.[5] In all these cases, pRh was found to have a tubular or fibril morphology.

Hollow polymeric particles have stimulated an increasing interest in the area of material science because of their large surface area, tunable particle diameter and shell thickness, and low permeability and density. Owing to these properties, the nanosized spheres find applications in medicine, biology, and industry, for instance, as nano-/microreaction vessels, targeted drug delivery, controlled release, photocatalysis, and synthetic pigments at industrial scale.[6−8] Because of our interest in these applications, we have been exploring ways to selectively synthesize polymeric nano-/microspheres in good yield and under mild reaction conditions.

To the best of our knowledge, there are no reports for the direct one-pot, green synthesis of pRh nano-/microspheres. In this work, we report a facile, single-step, green synthesis of pRh core−shell micro-/nanospheres, with copper acetate as the oxidizing agent (Scheme 1). The polymerization of Rh is carried out using a microwave synthetic protocol under mild reaction conditions. The reaction selectively produces pRh microspheres, and it does not require templates to control the morphology. Moreover, this transformation can be carried out in green solvents such as water or ethanol. The composite oxidants $KMnO_4$ and $Cu(OAc)_2$ exhibited faster formation processes and almost a quantitative conversion of Rh to pRh nano-/microspheres. However, in the absence of $Cu(OAc)_2$, $KMnO_4$, being a strong oxidant, produces a porous non-

Received: July 9, 2018
Accepted: August 29, 2018
Published: September 11, 2018

DOI: 10.1021/acsomega.8b01588
ACS Omega 2018, 3, 10974−10979

Scheme 1. Reaction of Rhodanine to Produce Polyrhodanine−Cu(II) Complex Nanospheres

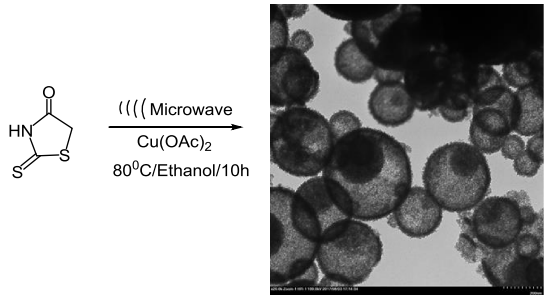

spherical pRh composite material. In addition, we demonstrate in this article the utility of pRh micro-/nanospheres as adsorbents for the methyl orange (MO) dye in aqueous solutions.

2. RESULTS AND DISCUSSION

The preliminary experiments were carried out under various reaction conditions and molar ratios to examine the morphological evolution of the pRh polymers in the presence of copper acetate. We observed an instant reaction of the ethanolic solution of rhodanine monomer with equimolar amounts of copper(II) acetate at room temperature (RT) to produce an olive green precipitate of the rhodanine−Cu(II) complex **P1**. The amount of the precipitate keeps increasing till 2 h of the reaction at RT or on heating the reaction mixture for 30 min. An idealized structure of the proposed complex is shown in Scheme 2.

Scheme 2. Reaction of Rhodanine with Copper Acetate to Produce Olive Green Rhodanine−Cu(II) Complex

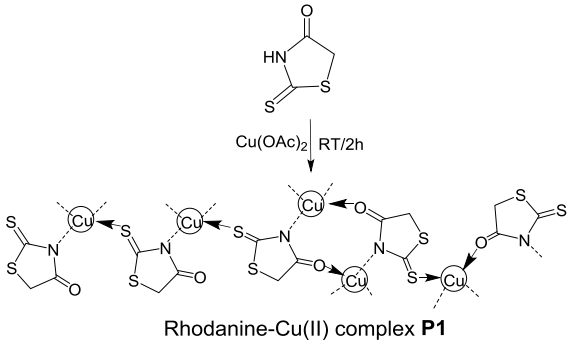

The initial reaction in this oxidative oligo-/polymerization process between Rh and Cu^{2+} takes place, in which a complex of Rh with copper is formed by the deprotonation of the amide group and coordination of the nitrogen, sulfur, and/or carbonyl group with the Cu(II) ion to produce the rhodanine−Cu(II) complex **P1**. This conclusion was drawn from a comparative Fourier transform infrared (FT-IR) spectroscopy analysis of the pristine Rh and pRh−$Cu^{(II)}$ complex (Figure 1) as well as from the precedent literature, where pRh has been isolated and characterized by IR spectroscopy.[3] The FT-IR analysis clearly indicates the deprotonation of the NH bond, as evidenced by the disappearance of the bands associated with NH (3172, 3087, and 1439 cm^{-1}). In addition, a red shift occurs in the C═S band (from 1075 cm^{-1} in Rh to 1018 cm^{-1} in the Rh−$Cu^{(II)}$

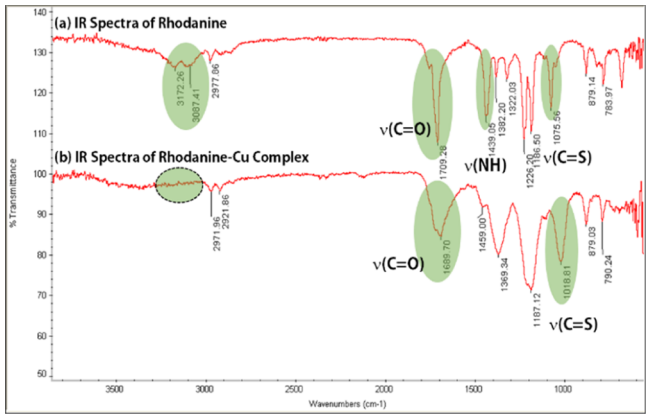

Figure 1. IR spectroscopy of rhodanine and rhodanine−Cu(II) complex.

complex) and in the carbonyl (C═O) band (from 1709 in Rh to 1689 cm^{-1} Rh−$Cu^{(II)}$ complex). These data suggest several modes of coordination (N, S, O) of Rh with Cu(II) in the complex.[9]

The morphological analysis of the olive green complex **P1** was also performed using scanning electron microscopy (SEM) and transmission electron microscopy (TEM) (Figure 2).

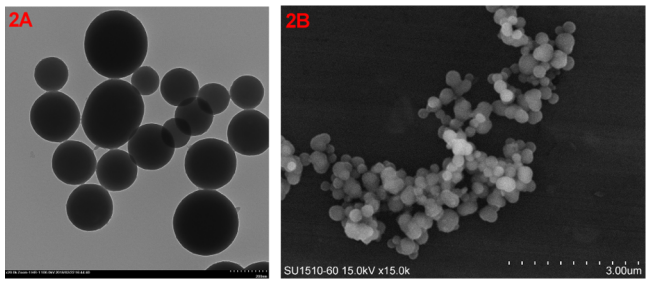

Figure 2. TEM (A) and SEM (B) analyses of the olive green rhodanine−Cu(II) complex.

These analyses provided further insights into the structural features of the Cu−Rh complex **P1**. To our surprise, we found that the morphology of the complex **P1** is spherical, and the size of these microspheres was found to be in the range of 20−200 nm. It was observed that the same products were obtained when the reaction was carried out in water. In the case of water as the solvent, the particles were found to be smaller in diameter and visually more porous than the particles obtained in the case of ethanol as the solvent.

To fully investigate this process, further reactions of the **P1** complex were investigated in detail. After the initial formation of the complex **P1** (Scheme 3), if the reaction was continued in the microwave at 80 °C for 10 h, a black precipitate was obtained, which was centrifuged, separated, and washed several times with ethanol and air-dried. In the FT-IR spectra of this product, signal broadening is observed, which is attributed to the formation of the pRh polymer.[3] Because of the polymerization, a new set of peaks at 1559 cm^{-1} of C═N stretching vibration and 1652 cm^{-1} for C═C stretching vibration also appears. The peak at 1407 cm^{-1} was assigned to the $C{=}N^{+}$ stretching and the peak at 1181 cm^{-1} is assigned to $C{-}O^{-}$. Similar to FT-IR, Raman analysis shows broadening of signals because of polymerization. Some noteworthy peaks in the polymer include 1559, 1098, and 558 cm^{-1} for the N−C

DOI: 10.1021/acsomega.8b01588
ACS Omega 2018, 3, 10974−10979

Scheme 3. Synthesis of Core−Shell pRh

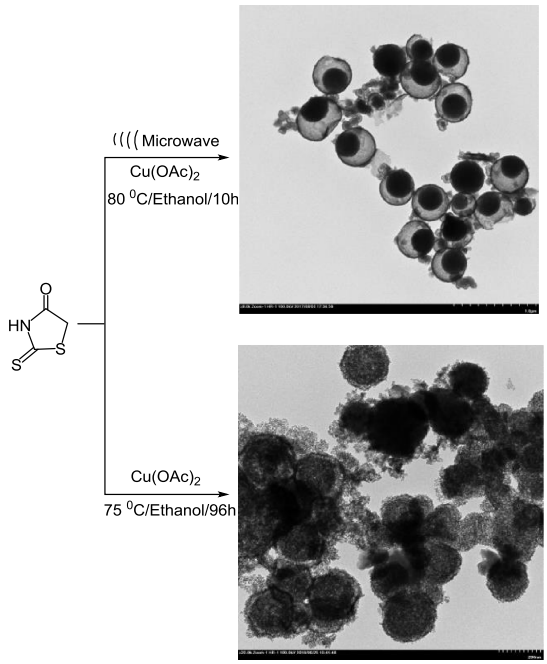

stretch; 447 cm^{-1} for the C−S stretch and C═S stretch for out-of-plane deformation (see the Supporting Information).

The UV−vis spectra of Rh in ethanol display two bands, with the maxima in the ranges 230−274 and 295−308 nm, which are associated with three chromophore groups (Figure 3): the thioamide group in the 230−274 nm range and the

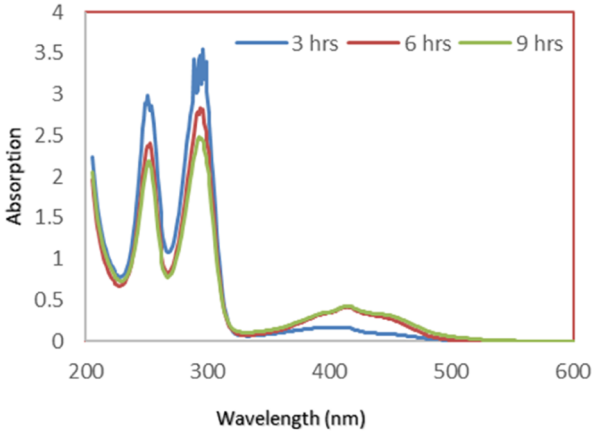

Figure 3. Monitoring of the formation of the core−shell pRh nanoparticles obtained in a microwave by UV−vis spectroscopy.

amide and dithio groups in the 295−308 nm range. In Figure 3, the UV−vis plots of the soluble part of the reaction mixture are shown after 3, 6, and 9 h of the reaction in the microwave. It is quite evident that as the reaction proceeds, new broad absorption bands appear between the 360 and 580 nm maxima centered at 420 nm. The peak devolution of pRh in 1 M NaOH solution shows 360 nm due to n−p* transition, 520−580 nm Cu^0 Plasmon resonance and 460 nm originates from pRh backbone.[3] It should be pointed out that because of the poor solubility of the core−shell pRh, it is difficult to analyze or monitor the progress of this reaction via the UV−vis spectra.

The TEM and SEM studies were performed to elucidate the morphology of the pRh product. To our surprise, the morphology of the precursor complex **P1** was retained, but now the spheres were converted into the pRh core−shell nanospheres (Scheme 3 and Figure 4). It was observed that

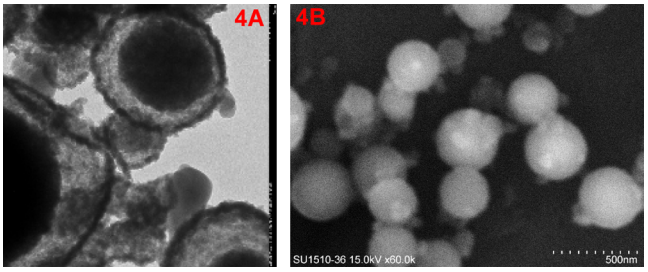

Figure 4. TEM (A) and SEM (B) micrographs of the core−shell pRh nanoparticles obtained in a microwave.

each sphere has a core with smooth surface and a shell with a rough outside surface. There was a dark inner solid core, an inner middle cavity which is lighter, and a dark outer shell (Figure 4A). According to earlier reports, pRh nanofibers with silver ions and electrochemical film formation on copper surfaces are known.[3,10] In our studies, the core−shell micro-/nanostructures were obtained by the simple copper(II)-promoted self-assembly method in green solvents such as ethanol. Similar structures were obtained when the reactions were carried out in water.

This template-free method can be scaled for large-scale pRh nanosphere synthesis without tedious synthesis and the complication of template removal. Though the detailed mechanistic studies are underway, our preliminary studies (see Scheme 4) indicate that at the initial stage of formation, the Rh−Cu(II) complex adopts the nano- and microsphere morphology, most probably driven by Cu-complexation to Rh. On heating the complex, in a microwave or under reflux conditions, Ostwald ripening process occurs. In this ripening process, the rhodanine in solution undergoes polymerization via the autocatalytic electrochemical pathway on the surface of the microspheres, creating a hard shell.[11] The complex inside the solid sphere has a strong tendency to dissolve slowly as the reaction progresses and deposits on the surface of the sphere, leading to the formation of core−shell structures as a black precipitate. The proposed mechanism is supported by the fact that the complex structures are solid spheres, whereas the TEM images taken at different time intervals of the reaction mixtures show spheres with and without the core−shell structures till the reaction is complete. The TEM images taken at different time intervals are shown in the Supporting Information.

To investigate the generality of the core−shell nanosphere formation, this reaction was investigated in the presence of strong oxidants such as $KMnO_4$. As $KMnO_4$ is a comparatively stronger oxidant, it can be expected to speed up the polymerization reaction. To examine this hypothesis, $KMnO_4$ and rhodanine were reacted under identical reaction conditions, but without $Cu(OAc)_2$ (Scheme 5). This reaction was faster, and a colorless solution with black precipitate was obtained after 4 h of reaction. As expected, pRh formation was observed. However, to our surprise, when TEM analysis was performed, it was found that the resulting pRH morphology was not that of the microspheres.

DOI: 10.1021/acsomega.8b01588
ACS Omega 2018, 3, 10974−10979

Scheme 4. Mechanistic Proposal and Cartoon Illustration of the Formation of Core−Shell Nanostructures

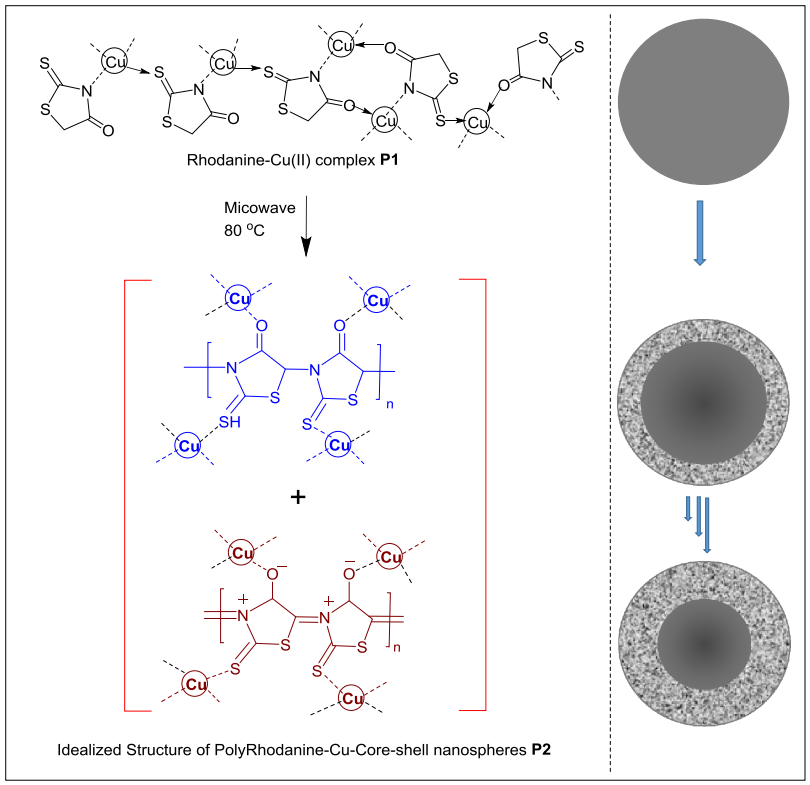

Scheme 5. Reaction of Rhodanine with $KMnO_4$

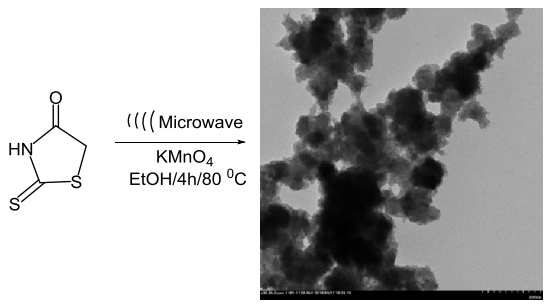

This led us to examine the synthesis of pRh in the presence of the composite catalyst $Cu(OAc)_2$ and $KMnO_4$ in ethanol. This time again, the reaction was as fast as before and showed a complete precipitation of pRh after 4 h of heating in the microwave. The black precipitate product was removed via centrifugation, and the remaining supernatant solution was examined via UV−vis spectroscopy. The UV−vis analysis indicated a marked decrease in the concentration of Rh monomer in the solution, indicating the complete conversion to polyrhodanine. When this black solid was examined by TEM, the same core−shell structures were observed. These results clearly indicated that pRh formation takes place via the redox process; however, the spherical polymer can only be generated in the presence of Cu(II) acetate.

In Table 1, various reaction conditions and morphologies of the resulting polyrhodanines are summarized.

To examine the utility of the pRh core−shell structures, the remediation of the dye-contaminated wastewater, one of the many green applications of these polyrhodanine particles, was considered. In addition, this investigation can have broad implications because the applications of dyes in food, cosmetics, textile, and paper industries lead to the leaching of dyes in wastewater streams. For example, MO dye is a known contaminant in industrial wastewater. We wanted to examine the suitability of the pRH nanoparticles for the removal of the MO dye from aqueous solutions. For this study, the pRH nanocomposite prepared according to the method in Section 3.3 (see the Experimental Section) was used. UV−vis spectroscopy was selected to monitor the MO absorption (Figure 5). In this preliminary study, to our surprise, we found that when the aqueous solution of MO was stirred with the pRH nanocomposite, within 3 h, about 80% of the MO dye was absorbed by the pRh nanocomposite. If the reaction was

Table 1. Synthesis of Polyrhodanine pRh under Different Reaction Conditions

entry	reactants	Rx conditions	morphology of pRh
1	Rh + $Cu(OAc)_2$ (1:1 molar ratio)	microwave, ethanol/9 h/80 °C	core−shell nanospheres
2	Rh + $Cu(OAc)_2$ (1:1 molar ratio)	ethanol/96 h/80 °C	core−shell nanospheres
3	Rh + $Cu(OAc)_2$ + $KMnO_4$ (1:1:1 molar proportion)	ethanol/4 h/80 °C	comparatively small core−shell nanospheres
4	Rh + $Cu(OAc)_2$ (1:1 molar proportion)	microwave, deionized H_2O/10 h/80 °C	core−shell nanospheres
5	Rh + $Cu(OAc)_2$ + $KMnO_4$ (1:1:1 molar proportion)	deionized water/2 h/80 °C	relatively small core−shell nanospheres
6	Rh + $KMnO_4$ (1:1 molar proportion)	ethanol/4 h/80 °C	no distinct morphology

DOI: 10.1021/acsomega.8b01588
ACS Omega 2018, 3, 10974−10979

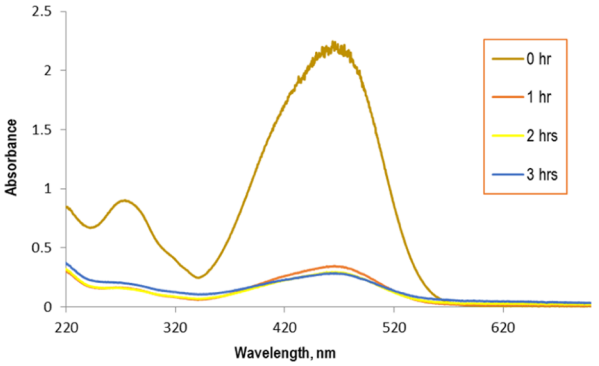

Figure 5. UV−vis spectroscopic analysis of the adsorption of methyl orange by polyrhodanine nanospheres at RT.

continued for longer times, the absorption remained around 80%. This facile absorption study bodes well for the application of the pRh nano-/microspheres. The detailed dye absorption studies are underway in our laboratories, and their results will be disclosed in due time.

3. EXPERIMENTAL SECTION

The detailed experimental procedures and analysis are provided in the Supporting Information.

3.1. Microwave Synthesis of pRh Core−Shell Nanoparticles with Copper Acetate. In a typical procedure, rhodanine monomer (0.2 mM) was dissolved in ethanol (15 mL) under stirring in a 20 mL Biotage microwave vial; then, copper(II) acetate (0.2 mM) was introduced into the rhodanine solution at RT. As soon as $Cu(OAc)_2$ was added to the stirred solution, a green precipitate of the Cu(II)−Rh complex was formed, which was then heated in a microwave at 80 °C for 10 h. During this period, the reaction was monitored intermittently by UV−vis and IR spectroscopy. After 9−10 h of the reaction, a black precipitate was obtained. This black precipitate was centrifuged, and the supernatant greenish yellow solution was carefully separated and discarded. The black solid was washed four times with 3 mL of ethanol and air-dried for 24 h. The elemental analysis of this solid was also performed. The CHN analysis indicated 8.16% C, 0.47% H, and 3.50% of N. The inductively coupled plasma−mass spectrometry analysis of the same sample showed that 55.9% of Cu was also present. A comparison to the expected C, H, N, and Cu percentage based on the idealized Cu-complexed polymer structure was found to be 8.95% C; 0.5% H; 3.48% N, and 55.24% of Cu. The same procedure was repeated using deionized water as the solvent.

3.2. Thermal Synthesis of pRh Core−Shell Nanoparticles with Copper Acetate. In a typical procedure, in a 150 mL two-neck round-bottom flask, rhodanine monomer (0.2 mM) was dissolved in ethanol (15 mL), and copper(II) acetate (0.2 mM) was introduced into the rhodanine solution at RT. As soon as $Cu(OAc)_2$ was added to the stirred solution, an olive green precipitate of the Cu(II)−Rh complex was formed, which was then heated in an oil bath at 75 °C. After 96 h of the reaction at 75 °C, a black precipitate was obtained. The black precipitate was centrifuged, and the supernatant solution was carefully separated and discarded. The solid black product was washed four times with 3 mL of ethanol, air-dried for 24 h, and analyzed. The same procedure was repeated using deionized water as the solvent.

3.3. Microwave Synthesis of pRh with Composite Catalysts. The rhodanine monomer (0.2 mM) was dissolved in ethanol (15 mL) under stirring in a 20 mL Biotage microwave vial, and copper(II) acetate (0.2 mM) was introduced into the rhodanine solution at RT. To the green suspension of the Cu(II)−Rh complex formed by the above reaction, potassium permanganate (0.2 mM) was added. This solution was heated in a microwave at 80 °C and intermittently analyzed by the UV−vis and IR spectra. The supernatant solution was colorless and a black precipitate was obtained after 4 h of the reaction. The reaction was deemed complete now, and the mixture was centrifuged. After centrifugation, a black solid was obtained, which was washed four times with 3 mL of ethanol and then air-dried for 24 h and analyzed. The IR and UV−vis analyses of the supernatant liquid showed only traces of unreacted Cu(II)−Rh complex or polyrhodanine.

3.4. Synthesis of pRh with $KMnO_4$ as Oxidant. The rhodanine monomer (0.2 mM) was dissolved in ethanol (15 mL) under stirring in a 20 mL Biotage microwave vial, and potassium permanganate (0.2 mM) was added to this solution. No precipitation/suspension formation occurred at RT, and after heating the solution at 80 °C in the microwave for 4 h, a black precipitate was obtained. The solid was centrifuged, washed four times with 3 mL of ethanol, and air-dried for 24 h.

3.5. Adsorption of MO by pRh. In a 50 mL round-bottom flask, 20 mL of 0.00303 M MO solution prepared by dissolving 0.001 mol of MO in 0.330 L of deionized water was added under stirring at RT, and 0.0140 g of pRh was added to this solution. The suspension was stirred at RT and monitored by UV−vis spectroscopy. For UV−vis measurements, a 3 mL aliquot of the reaction mixture was taken out every hour and centrifuged. The supernatant liquid was collected, and 0.2 mL of this solution was diluted with 3.4 mL of deionized water for every UV−vis measurement.

■ ASSOCIATED CONTENT

Supporting Information

The Supporting Information is available free of charge on the ACS Publications website at DOI: 10.1021/acsomega.8b01588.

Experimental and analytical details; IR of the rhodanine and olive green rhodanine−Cu complex; IR of the rhodanine and polyrhodanine nanospheres obtained under microwave conditions; monitoring of the polyrhodanine nanosphere formation under microwave conditions by UV−vis spectroscopy; TEM and SEM of polyrhodanine nanospheres obtained under microwave conditions; and overlay of Raman spectra of rhodanine and polyrhodanine nanospheres obtained under microwave conditions (PDF)

■ AUTHOR INFORMATION

Corresponding Authors

*E-mail: Mchauhan@qcc.cuny.edu (M.C.).
*E-mail: Chauhanbps@wpunj.edu (B.P.S.C.).

ORCID

Bhanu P. S. Chauhan: 0000-0002-4816-5643

Notes

The authors declare no competing financial interest.

DOI: 10.1021/acsomega.8b01588
ACS Omega 2018, 3, 10974−10979

■ ACKNOWLEDGMENTS

B.P.S.C. acknowledges the ART and student support from the college of Science and Health. M.C. acknowledges research support from CUNY-Queensborough Community College.

■ REFERENCES

(1) (a) Gomez-Romero, P. Hybrid Organic−Inorganic Materials—In Search of Synergic Activity. *Adv. Mater.* **2001**, *13*, 163−174. (b) Zhou, Y.; Itoh, H.; Uemura, T.; Naka, K.; Chujo, Y. Synthesis of Novel Stable Nanometer-Sized Metal (M = Pd, Au, Pt) Colloids Protected by a π-Conjugated Polymer. *Langmuir* **2002**, *18*, 277−283. (c) Greenham, N. C.; Peng, X.; Alivisatos, A. P. Charge Separation and Transport in Conjugated-Polymer/Semiconductor-Nanocrystal Composites Studied by Photoluminescence Quenching and Photoconductivity. *Phys. Rev. B* **1996**, *54*, 17628−17637. (d) Colvin, V. L.; Schlamp, M. C.; Alivisatos, A. P. Light-Emitting Diodes Made from Cadmium Selenide Nanocrystals and a Semiconducting Polymer. *Nature* **1994**, *370*, 354−357. (e) Miller, E. K.; Brabec, C. J.; Neugebauer, H.; Heeger, A. J.; Sariciftci, N. S. Polarized Doping-Induced Infrared Absorption in Highly Oriented Conjugated Polymers. *Chem. Phys. Lett.* **2001**, *335*, 23−26. (f) Pang, X.; He, Y.; Jung, J.; Lin, Z. 1D Nanocrystals with Precisely Controlled Dimensions, Compositions, and Architectures. *Science* **2016**, *353*, 1268−1272. (g) Pang, X.; Zhao, L.; Han, W.; Xin, X.; Lin, Z. A General and Robust Strategy for the Synthesis of Nearly Monodisperse Colloidal Nanocrystals. *Nat. Nanotechnol.* **2013**, *8*, 426−431.

(2) (a) Gualtieri, M.; Bastide, L.; Villain-Guillot, P.; Michaux-Charachon, S.; Latouche, J.; Leonetti, J.-P. In Vitro Activity of a New Antibacterial Rhodanine Derivative against Staphylococcus Epidermidis Biofilms. *J. Antimicrob. Chemother.* **2006**, *58*, 778−783. (b) Kumar, G.; Parasuraman, P.; Sharma, S. K.; Banerjee, T.; Karmodiya, K.; Surolia, N.; Surolia, A. Discovery of a Rhodanine Class of Compounds as Inhibitors ofPlasmodium falciparumEnoyl-Acyl Carrier Protein Reductase. *J. Med. Chem.* **2007**, *50*, 2665−2675. (c) Tang, E.; Yang, G.; Yin, J. Studies on the Synthesis of 5-(p-Aminobenzylidene)-Rhodanine and Its Properties. *Spectrochim. Acta, Part A* **2003**, *59*, 651−656. (d) Sortino, M.; Delgado, P.; Juárez, S.; Quiroga, J.; Abonía, R.; Insuasty, B.; Nogueras, M.; Rodero, L.; Garibotto, F. M.; Enriz, R. D.; et al. Synthesis and Antifungal Activity of (Z)-5-Arylidenerhodanines. *Bioorg. Med. Chem.* **2007**, *15*, 484−494. (e) Solmaz, R.; Kardas, G.; Yazici, B.; Erbil, M. Inhibition Effect of Rhodanine for Corrosion of Mild Steel in Hydrochloric Acid Solution. *Prot. Met.* **2005**, *41*, 581−585.

(3) (a) Kardaş, G.; Solmaz, R. Electrochemical Synthesis and Characterization of a New Conducting Polymer: Polyrhodanine. *Appl. Surf. Sci.* **2007**, *253*, 3402−3407. (b) Kong, H.; Song, J.; Jang, J. One-Step Preparation of Antimicrobial Polyrhodanine Nanotubes with Silver Nanoparticles. *Macromol. Rapid Commun.* **2009**, *30*, 1350−1355. (c) Kong, H.; Jang, J. Synthesis and Antimicrobial Properties of Novel Silver/Polyrhodanine Nanofibers. *Biomacromolecules* **2008**, *9*, 2677−2681.

(4) (a) Tang, J.; Song, Y.; Tanvir, S.; Anderson, W. A.; Berry, R. M.; Tam, K. C. Polyrhodanine Coated Cellulose Nanocrystals: A Sustainable Antimicrobial Agent. *ACS Sustainable Chem. Eng.* **2015**, *3*, 1801−1809. (b) Song, J.; Kim, H.; Jang, Y.; Jang, J. Enhanced Antibacterial Activity of Silver/Polyrhodanine-Composite-Decorated Silica Nanoparticles. *ACS Appl. Mater. Interfaces* **2013**, *5*, 11563−11568.

(5) (a) Song, J.; Oh, H.; Kong, H.; Jang, J. Polyrhodanine Modified Anodic Aluminum Oxide Membrane for Heavy Metal Ions Removal. *J. Hazard. Mater.* **2011**, *187*, 311−317. (b) Owczarek, E.; Adamczyk, L. Electrochemical and Anticorrosion Properties of Bilayer Polyrhodanine/Isobutyltriethoxysilane Coatings. *J. Appl. Electrochem.* **2016**, *46*, 635−643.

(6) (a) Caruso, F.; Caruso, R. A.; Möhwald, H. Nanoengineering of Inorganic and Hybrid Hollow Spheres by Colloidal Templating. *Science* **1998**, *282*, 1111−1114. (b) Deng, Z.; Chen, M.; Zhou, S.; You, B.; Wu, L. A Novel Method for the Fabrication of Monodisperse Hollow Silica Spheres. *Langmuir* **2006**, *22*, 6403−6407. (c) Cheng, X.; Chen, M.; Wu, L.; Gu, G. Novel and Facile Method for the Preparation of Monodispersed Titania Hollow Spheres. *Langmuir* **2006**, *22*, 3858−3863. (d) Hu, J.; Chen, M.; Fang, X.; Wu, L. Fabrication and Application of Inorganic Hollow Spheres. *Chem. Soc. Rev.* **2011**, *40*, 5472−5491. (e) Zhang, K.; Zhang, X.; Chen, H.; Chen, X.; Zheng, L.; Zhang, J.; Yang, B. Hollow Titania Spheres with Movable Silica Spheres Inside. *Langmuir* **2004**, *20*, 11312−11314. (f) Lv, H.; Lin, Q.; Zhang, K.; Yu, K.; Yao, T.; Zhang, X.; Zhang, J.; Yang, B. Facile Fabrication of Monodisperse Polymer Hollow Spheres. *Langmuir* **2008**, *24*, 13736−13741. (g) Chen, T.; Colver, P. J.; Bon, S. A. F. Organic-Inorganic Hybrid Hollow Spheres Prepared from TiO2-Stabilized Pickering Emulsion Polymerization. *Adv. Mater.* **2007**, *19*, 2286−2289. (h) Yang, M.; Wang, G.; Yang, Z. Synthesis of Hollow Spheres with Mesoporous Silica Nanoparticles Shell. *Mater. Chem. Phys.* **2008**, *111*, 5−8. (i) Yang, M.; Ma, J.; Zhang, C.; Yang, Z.; Lu, Y. General Synthetic Route toward Functional Hollow Spheres with Double-Shelled Structures. *Angew. Chem. Int. Ed.* **2005**, *44*, 6727−6730. (j) Li, L.; Ding, J.; Xue, J. Macroporous Silica Hollow Microspheres as Nanoparticle Collectors. *Chem. Mater.* **2009**, *21*, 3629−3637. (k) Chen, Z.; Cui, Z.-M.; Cao, C.-Y.; He, W.-D.; Jiang, L.; Song, W.-G. Temperature-Responsive Smart Nanoreactors: Poly(N-Isopropylacrylamide)-Coated Au@Mesoporous-SiO2 Hollow Nanospheres. *Langmuir* **2012**, *28*, 13452−13458. (l) Han, J.; Fang, P.; Dai, J.; Guo, R. One-Pot Surfactantless Route to Polyaniline Hollow Nanospheres with Incontinuous Multicavities and Application for the Removal of Lead Ions from Water. *Langmuir* **2012**, *28*, 6468−6475. (m) Han, J.; Dai, J.; Guo, R. Highly Efficient Adsorbents of Poly(o-Phenylenediamine) Solid and Hollow Sub-Microspheres towards Lead Ions: A Comparative Study. *J. Colloid Interface Sci.* **2011**, *356*, 749−756. (n) Yang, J.; Lee, J.; Kang, J.; Lee, K.; Suh, J.-S.; Yoon, H.-G.; Huh, Y.-M.; Haam, S. Hollow Silica Nanocontainers as Drug Delivery Vehicles. *Langmuir* **2008**, *24*, 3417−3421. (o) Wang, Z.; Wu, L.; Chen, M.; Zhou, S. Facile Synthesis of Superparamagnetic Fluorescent Fe3O4/ZnS Hollow Nanospheres. *J. Am. Chem. Soc.* **2009**, *131*, 11276−11277.

(7) (a) Zhu, Y.; Hu, D.; Wan, M. X.; Jiang, L.; Wei, Y. Conducting and Superhydrophobic Rambutan-like Hollow Spheres of Polyaniline. *Adv. Mater.* **2007**, *19*, 2092−2096. (b) Zhang, L.; Wan, M. Self-Assembly of Polyaniline-From Nanotubes to Hollow Microspheres. *Adv. Funct. Mater.* **2003**, *13*, 815−820.

(8) Tan, Y.; Bai, F.; Wang, D.; Peng, Q.; Wang, X.; Li, Y. Template-Free Synthesis and Characterization of Single-Phase Voided Poly(o-Anisidine) and Polyaniline Colloidal Spheres. *Chem. Mater.* **2007**, *19*, 5773−5778.

(9) Marzec, K. M.; Gawel, B.; Lasocha, W.; Proniewicz, L. M.; Malek, K. Interaction between Rhodanine and Silver Species on a Nanocolloidal Surface and in the Solid State. *J. Raman Spectrosc.* **2010**, *41*, 543−552.

(10) Honesty, N. R.; Kardaş, G.; Gewirth, A. A. Investigating Rhodanine Film Formation on Roughened Cu Surfaces with Electrochemical Impedance Spectroscopy and Surface-Enhanced Raman Scattering Spectroscopy. *Corros. Sci.* **2014**, *83*, 59−66.

(11) Lou, X. W. D.; Archer, L. A.; Yang, Z. Hollow Micro-/Nanostructures: Synthesis and Applications. *Adv. Mater.* **2008**, *20*, 3987−4019.

DOI: 10.1021/acsomega.8b01588
ACS Omega 2018, 3, 10974−10979